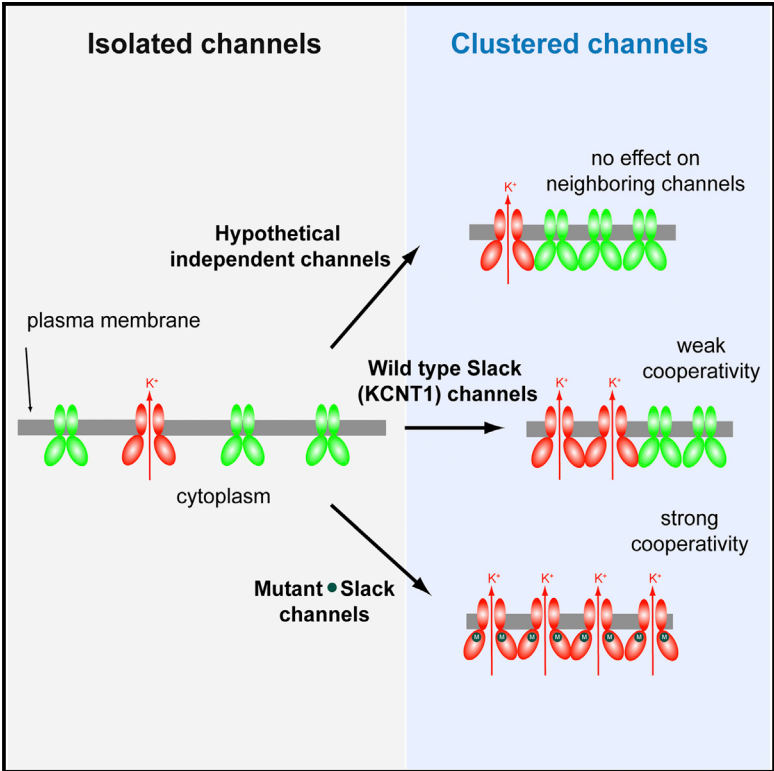# Human Slack Potassium Channel Mutations Increase Positive Cooperativity between Individual Channels

Graphical Abstract

Authors

Grace E. Kim, Jack Kronengold, ...,
Rima Nabbout, Leonard K. Kaczmarek

Correspondence

leonard.kaczmarek@yale.edu

In Brief

Slack KCNT1 channels regulate how neurons respond to sustained stimulation. Kim et al. characterized nine KCNT1 mutations found in epilepsy patients with severe intellectual disabilities and showed that, in isolation, channel behavior is unaltered. However, in groups, mutant channels interact with each other abnormally, increasing current that flows through the channels.

Highlights

Slack KCNT1 mutations are found in three different epilepsy syndromes

Abnormal interactions between individual mutants greatly increase K⁺ current

Cooperativity enhances K⁺ current even in a mutant with reduced channel conductance

The same mutation can produce different forms of epilepsy in different individuals

CellPress

Human Slack Potassium Channel Mutations Increase Positive Cooperativity between Individual Channels

Grace E. Kim,[1,2,9] Jack Kronengold,[1,9] Giulia Barcia,[3] Imran H. Quraishi,[4] Hilary C. Martin,[5] Edward Blair,[6] Jenny C. Taylor,[7] Olivier Dulac,[3] Laurence Colleaux,[8] Rima Nabbout,[3,10] and Leonard K. Kaczmarek[1,2,10,*]
[1]Department of Pharmacology, Yale University, New Haven, CT 06520, USA
[2]Department of Cellular and Molecular Physiology, Yale University, New Haven, CT 06520, USA
[3]Department of Pediatric Neurology, Centre de Reference Epilepsies Rares, Hôpital Necker-Enfants Malades, Assistance Publique-Hôpitaux de Paris, 75015 Paris, France
[4]Comprehensive Epilepsy Center, Department of Neurology, Yale University, New Haven, CT 06520, USA
[5]Wellcome Trust Centre for Human Genetics, University of Oxford, Oxford OX3 7BN, UK
[6]Oxford University Hospitals Trust, Oxford OX3 9DU, UK
[7]Oxford Biomedical Research Centre, Wellcome Trust Centre for Human Genetics, University of Oxford, Oxford OX3 7BN, UK
[8]INSERM U781, Université Paris Descartes, Sorbonne Paris Cité, Institut Imagine, Hôpital Necker-Enfants Malades, 75015 Paris, France
[9]Co-first author
[10]Co-senior author
*Correspondence: leonard.kaczmarek@yale.edu
http://dx.doi.org/10.1016/j.celrep.2014.11.015

SUMMARY

Disease-causing mutations in ion channels generally alter intrinsic gating properties such as activation, inactivation, and voltage dependence. We examined nine different mutations of the KCNT1 (Slack) Na^+-activated K^+ channel that give rise to three distinct forms of epilepsy. All produced many-fold increases in current amplitude compared to the wild-type channel. This could not be accounted for by increases in the intrinsic open probability of individual channels. Rather, greatly increased opening was a consequence of cooperative interactions between multiple channels in a patch. The degree of cooperative gating was much greater for all of the mutant channels than for the wild-type channel, and could explain increases in current even in a mutant with reduced unitary conductance. We also found that the same mutation gave rise to different forms of epilepsy in different individuals. Our findings indicate that a major consequence of these mutations is to alter channel-channel interactions.

INTRODUCTION

The *KCNT1* gene encodes the Na^+-activated K^+ channel Slack (also known as Slo2.2). Mutations in *KCNT1* have been found in three different epilepsy syndromes (Barcia et al., 2012; Heron et al., 2012; Ishii et al., 2013; Martin et al., 2014): migrating malignant partial seizures in infancy (MMPSI) (Barcia et al., 2012; Ishii et al., 2013), autosomal dominant nocturnal frontal lobe epilepsy (ADNFLE) (Heron et al., 2012), and Ohtahara syndrome (OS) (Martin et al., 2014). In each of these cases, the patients with *KCNT1* mutations have a very high occurrence of severe mental and intellectual disability. When some of the known mutations were expressed in *Xenopus* oocytes, all mutations generated currents greater than those obtained with wild-type (WT) Slack channels (Barcia et al., 2012; Martin et al., 2014; Milligan et al., 2014). Although two mutations that produce MMPSI resulted in a 2- to 3-fold increase in current that mimics the activating effects of protein kinase C phosphorylation of the channel (Barcia et al., 2012), a mutation that produces OS showed a much greater increase in current (Martin et al., 2014), suggesting that other mechanisms must be involved. No change in the sensitivity of the mutant channels to Na^+ ions has been found (Barcia et al., 2012). Thus, it remains unknown whether yet another mechanism contributes to the change in channel activity, or whether the mutants share any common mechanisms for increased current.

We have now expressed nine of the previously published mutations in the Slack channel and characterized their macroscopic currents, levels of protein expression, and gating behavior at the single-channel level. These nine mutations account for 27 out of the 31 epilepsy cases attributed to *KCNT1* mutations. We have found that the mutations cause minimal changes in the gating of individual ion channels, but greatly increase the cooperativity in channel gating that is detected in clusters of multiple channels.

RESULTS

Clinical Characteristics of Patients with *KCNT1* Mutations

The clinical characteristics of the 16 patients (ten with MMPSI, five with ADNFLE, and one with OS) included in this study are

summarized in Table 1. All of the MMPSI patients showed pharmacoresistance and acquired microcephaly, although epilepsy onset ranged from 1 day of life to 2.5 months. They also developed a severe motor and cognitive delay. Among the ADNFLE patients, patient 10 in particular presented with a severe form, with first onset of seizure (nocturnal hypermotor seizures) occurring at 3 years. To date (at age 23 years), patient 10's seizures remain pharmacoresistant and frequent. Four mutations from families with ADNFLE (Heron et al., 2012) were also included in our analysis. Some members of these families had a more severe phenotype that deviated from classical ADNFLE; i.e., earlier seizure onset with more pharmacoresistant epilepsy that led to intellectual disability and various psychiatric disorders (Table 1). Patient 16 had OS that presented at day 1 with spasms and focal seizures, and a burst suppression pattern on EEG, resulting in profound developmental delay (Martin et al., 2014).

Three new patients (two with MMPSI and one with ADNFLE) were analyzed in this study. Both MMPSI patients had mutations considered to be deleterious, inducing a change in a conserved amino acid (c.2800G > A, hA934T in patient 6 and c.1193G > A, hR398Q in patient 11). The same hA934T mutation was also found in multiple, unrelated MMPSI patients (Barcia et al., 2012), and the hR398Q mutation was found in a family with ADNFLE (Heron et al., 2012). Similarly, the mutation c.862G > A, hG288S, which was previously found in two MMPSI patients (Ishii et al., 2013), was also present in patient 10, an ADNFLE patient.

KCNT1 Point Mutations Lead to Increased Channel Activity with Minor Changes in Protein Expression

We previously characterized two KCNT1 or Slack mutant channels, hR428Q and hA934T, which correspond to R409Q and A913T, respectively, in the rat, using two-electrode voltage clamping (Barcia et al., 2012). All of the mutants listed in Table 1 and Figure 1A were generated likewise using the rat clone, which shares 92% sequence homology to the human clone, and are referred to using the rat amino acid numbering system. We studied channels in *Xenopus laevis* oocytes because their controlled expression system allowed us to make cross-mutation comparisons of channel expression. The current amplitude for WT Slack increased slowly for ≥ 4 days after injection (Figures 1B and 1C). When the peak current amplitude was compared at the physiological membrane potential of +20 mV, all mutants had significantly greater currents compared with WT Slack. There was a wide range of fold increases in channel activity, and for some mutants (e.g., R455H), the currents were already too large to quantify without saturation of the clamp amplifier 2 days after cRNA injection (Figure 1B). For this reason, we measured the peak currents of WT Slack and the mutants 1, 2, or 4 days after injection (Figures 1B and 1C). We found no correlation between the fold increase in channel activity and the type of epilepsy. This finding is consistent with the fact that some mutations, such as R379Q and G269S (Table 1; Figure 1A), are found in both MMPSI and ADNFLE patients.

To determine whether the increases in peak current amplitude resulted from increases in channel protein expression, we compared Slack protein abundance in membrane fractions by immunoblotting with an antibody that recognizes the N terminus

of the channel (Bhattacharjee et al., 2002). Use of this antibody ensured that the C-terminal mutants would not alter antibody recognition of the protein. Oocytes were homogenized after the completion of each voltage clamp. Densitometry of Slack bands, when normalized to the loading control Na$^+$/K$^+$ ATPase, revealed that changes in channel abundance were very minor and bore no correlation to the increase in current (Figure 2A). Only for the mutations A945T and G269S were the protein levels increased by ~2-fold, and these levels do not explain the >13-fold increases in current (Figure 1C; Martin et al., 2014). Overall, changes in the levels of Slack protein failed to correlate with the increases in channel activity for any of the three types of epilepsy.

A Subset of Slack Mutants Are Left-Shifted in Their Voltage Dependence

Slack channels are voltage dependent, with an increasing open probability (Po) at positive potentials (Joiner et al., 1998; Yuan et al., 2003). Therefore, a leftward shift in voltage dependence can increase currents at membrane potentials closer to neuronal resting potentials. We compared the voltage dependence of each mutant with that of WT Slack, and found that the majority of the mutants for MMPSI and ADNFLE had current-voltage relations identical to those of the WT channel (Figures 2C and 2D). A comparison of the normalized voltage-clamp traces of the MMPSI R455H and ADNFLE R907C mutants with those of the WT, however, revealed that both mutants showed a significant increase in channel activation at hyperpolarized membrane potentials (Figures 2B–2D). Although this change in voltage dependence may contribute to the observed increases in current, the degree to which this mechanism alone could enhance current (20%–30% at +20 mV) was not sufficient to explain the much larger increases in overall macroscopic current for these mutants.

### WT Slack Channels Have Both Low and High *P*o Patterns

To further compare the characteristics of the WT and mutant Slack channels, we carried out on-cell patch recordings from channels expressed in *Xenopus* oocytes. When patching from oocytes, one routinely observes a high degree of nonuniformity in channel number. Some membrane patches contain no channels, whereas other nearby patches constitute a "hot spot" containing variable numbers of channels. Figure 3 shows recordings obtained at −80 mV from representative patches containing apparently different numbers of WT Slack channels. Despite the identical experimental conditions, we found that there were two patterns of channel activity depending on whether the patches contained a lower (one to three) or higher (four or more) number of channels.

Figure 3A shows a typical recording at −80 mV in which predominantly only one open channel can be detected, and rare simultaneous openings of two channels are observed. As described previously, the channels are closed most of the time, with frequent openings to subconductance (SC) states (Brown et al., 2010). We term such low-*P*o patches "low-N" patches, and this recording is representative of all eight patches we recorded that contained WT Slack channels in which only one opening predominated. The corresponding all-points amplitude

Table 1. Clinical and Biophysical Characteristics of Human Mutant Slack Channels

Patient #	Mutation	Protein Human	Rat	Epilepsy Type	Age at Seizure Onset (Type)	Pharmaco resistance	Intellectual Delay	Microcephaly	Reference	Peak Current	Protein Expression	I/V	Conductance (i)
1	c.1283G > A	R428Q	R409Q	MMPSI	2 months	Y	Y	Y	Barcia et al., 2012	↑ 3-fold	NC[a]	NC[a]	fewer SC[b], same i[c]
2	c.1283G > A	R428Q	R409Q	MMPSI	1 day	Y	Y	Y	Barcia et al., 2012				
3	c.1283G > A	R428Q	R409Q	MMPSI	2 hr	Y	Y	Y	Barcia et al., 2012				
4	c.2800G > A	A934T	A913T	MMPSI	1 months	Y	Y	Y	Barcia et al., 2012	↑ 4-fold	NC	NC	fewer SC, same i
5	c.2800G > A	A934T	A913T	MMPSI	2 weeks	Y	Y	Y	McTague et al., 2013				
6	c.2800G > A	A934T	A913T	MMPSI	2.5 months (focal motor)	Y	Y	Y	–				
7	c.1421G > A	R474H	R455H	MMPSI	2 weeks	Y	Y	Y	Barcia et al., 2012	↑ 22-fold	NC	leftward shift	fewer SC, same i
8	c.862G > A	G288S	G269S	MMPSI	2 months (focal motor)	Y	Y	Y	Ishii et al., 2013	↑ 6-fold	NC	NC	fewer SC, 50% i
9	c.862G > A	G288S	G269S	MMPSI	2 months (focal motor with autonomic signs)	Y	Y	Y	Ishii et al., 2013				
10	c.862G > A	G288S	G269S	ADNFLE	3 years	Y	Y	N	–				
11	c.1193G > A	R398Q	R379Q	MMPSI	10 days (focal motor)	Y	Y	NK	–	↑ 3-fold	NC	NC	same i
12 (Fam.C)	c.1193G > A	R398Q	R379Q	ADNFLE	8.5 ± 6.4 years	0/4	2/4	NK	Heron et al., 2012				
13 (Fam.B)	c.2386T > C	Y796H	Y775H	ADNFLE	5.5 ± 2.1 years	2/4	2/4	NK	Heron et al., 2012	↑ 11-fold	NC	NC	same i
14 (Fam.D)	c.2688G > A	M896I	M875I	ADNFLE	9 years	1/1	1/1	NK	Heron et al., 2012	↑ 10-fold	reduced 2-fold	NC	80% i
15 (Fam.A)	c.2782C > T	R928C	R907C	ADNFLE	4.6 ± 5.9 years	5/6	3/6	NK	Heron et al., 2012	↑ 3-fold	NC	leftward shift	same i
16	c.2896G > A	A966T	R945T	OS	1 day	Y	Y	NK	Martin et al., 2014	↑ 13-fold	NC	NC	fewer SC, same i

[a]No change (NC).
[b]Indicates few occurrences of subconductance (SC) states.
[c]Indicates relative change in unitary conductance (i).
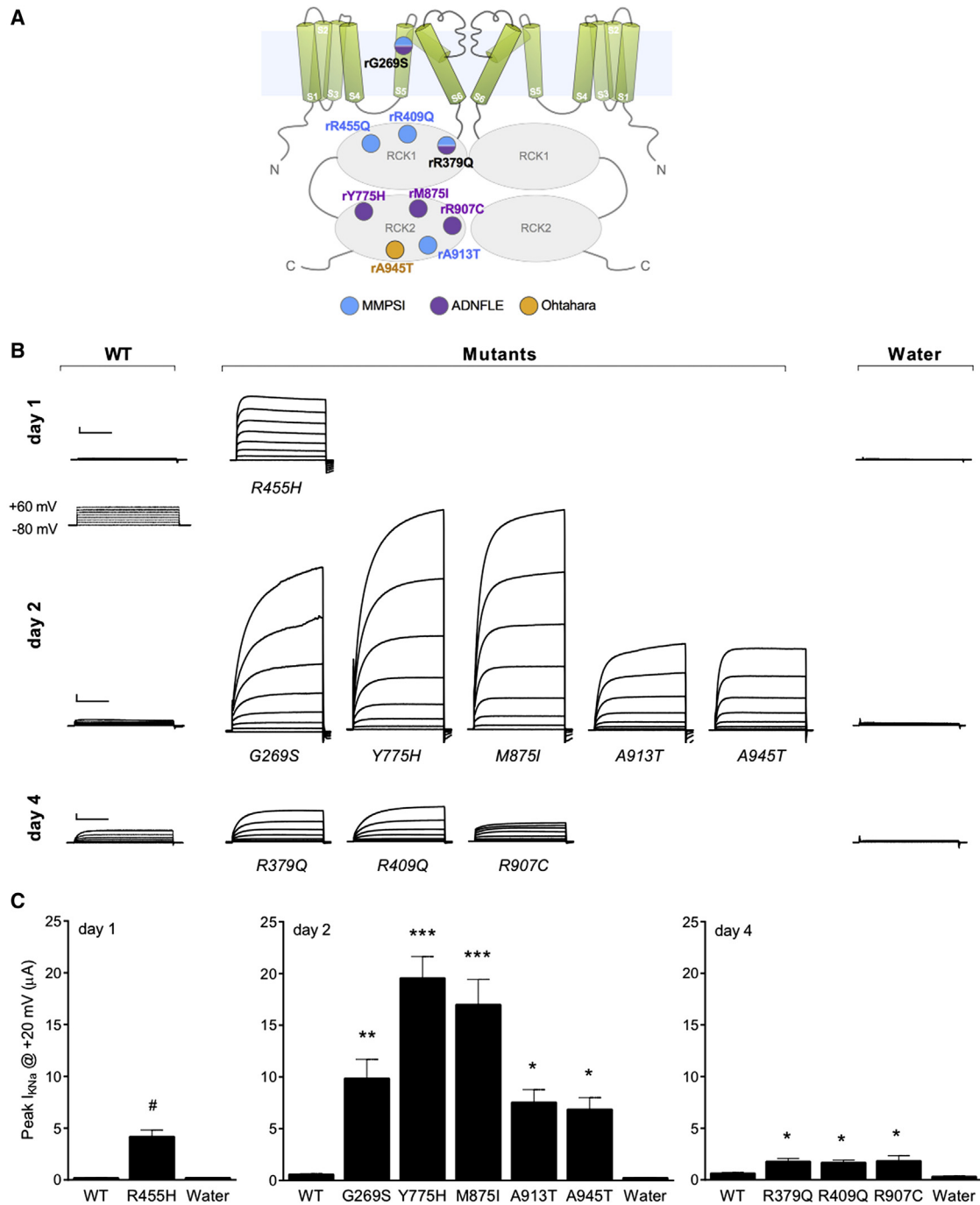
Figure 1. Slack Currents Are Increased by Mutations that Produce Epilepsy

(A) Diagram of two subunits of a Slack channel with the point mutations described in this study. Numbering refers to the rat Slack sequence. Positions of the mutations within the C-terminal "gating ring," containing two RCK domains (RCK1 and RCK2), are based on the low-resolution X-ray structure (Yuan et al., 2010).

(B) The voltage-clamp protocol and representative current traces show that peak current amplitude (I_{KNa}) is significantly increased in all mutants compared with the WT channel. *Xenopus* oocytes injected with cRNA encoding WT or mutant channels, or injected with water alone, were tested using a two-electrode voltage clamp on days 1, 2, or 4 following injection. Scale bars, 1 μA and 200 ms.

(C) Bar graphs quantifying the increase in mean peak current amplitude at +20 mV for all mutant channels compared with WT Slack (mean ± SEM, #$p < 0.01$ against WT, two-tailed Student's t test, n = 5; *$p < 0.05$, **$p < 0.01$, ***$p < 0.001$ against WT, one-way ANOVA with Tukey's post hoc test, n = 6–9 for all conditions).
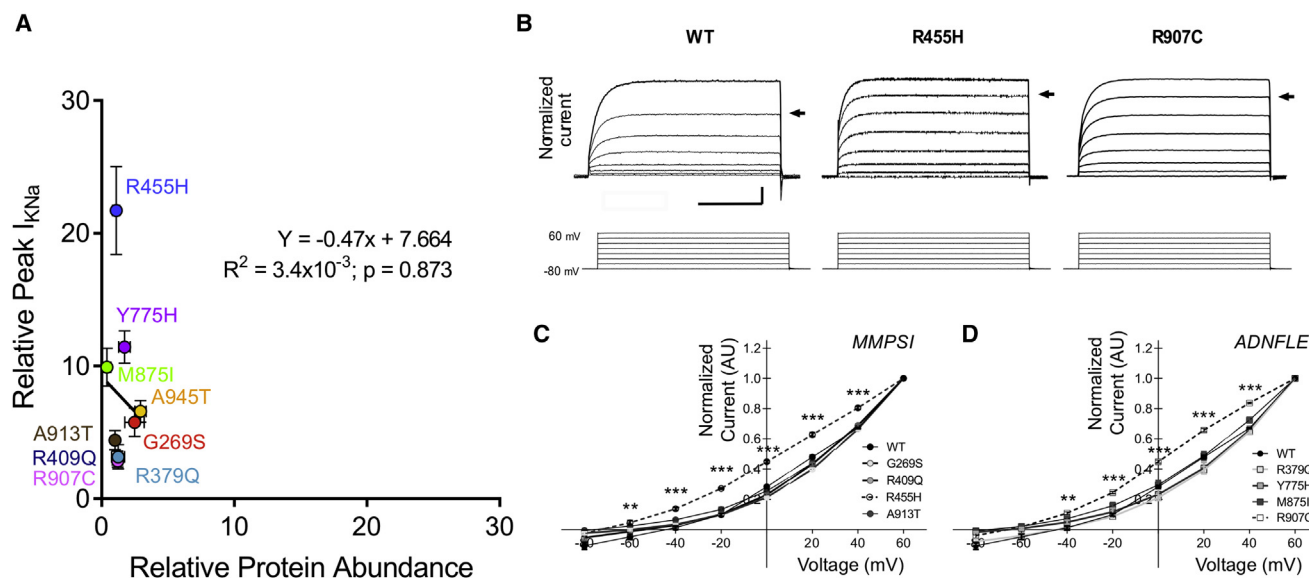
Figure 2. Channel Protein Expression Is Not Altered by Mutations

(A) Plot of the relative increase in peak I_{KNa} changes versus levels of Slack protein determined by densitometry of western blots of membrane fractions from oocytes homogenized immediately after the voltage-clamp experiments. A nonsignificant best fit (solid line) shows no relationship that can account for the increases in current (mean ± SEM).

(B) The voltage dependence of channel activation is shifted leftward in the R455H and R907C mutants. Representative traces for the WT and R455H and R907C mutants, normalized to their peak I_{KNa} at +60 mV, are shown. The shift in voltage dependence is made evident by the position of arrows lined up to the responses to test pulses at +40 mV. Scale bars represent 0.2 μm and 200 ms.

(C and D) Mean peak I_{KNa} at each of the command voltages, shown as an I/V plot for MMPSI (C) and ADNFLE (D) mutants. Current amplitudes were normalized to the peak I_{KNa} at +60 mV in all cases. The increase in relative channel activity was seen at voltages ≥ -60 mV and −40 mV for R455H (C) and R907C (D), respectively (mean ± SEM; **p < 0.01, ***p < 0.001 against WT, two-way ANOVA with Bonferroni's post hoc test, n = 5–10 for all points).

histogram derived from prolonged (2 min) recording of currents quantifies the low Po of the channel (Figure 3B). Given that there are likely to be at least two channels in this patch, the size of the peak corresponding to the single-channel opening level, O1, overestimates the true single-channel Po. Nevertheless, the amplitude of the O1 peak allows one to calculate the expected binomial distribution for multiple channels. If the channels are identical to those in a low-N patch and gate independently, then the probability that k channels will open out of a total of N should follow a binomial distribution. Figure 3C shows such a calculated distribution for a patch containing six channels.

Figure 3D shows a patch in which simultaneous openings of up to six Slack channels could be seen. We term such patches "high-N" patches, and this recording is representative of five such recordings in which four or more simultaneous openings were detected. The unitary conductances are identical to those seen in the low-N patches. However, an inspection of the all-points histogram for this patch (Figure 3E) shows that the channel Po does not reflect what one would expect to see based on the low-N patches. A comparison of the observed distribution of channel openings (Figure 3E) with that expected from the binomial distribution of six independently gating low-N channels (Figure 3C) shows a marked increase in open time and multiple simultaneous openings in the high-N patch.

We reasoned that the proximity of neighboring clustered channels in a high-N patch might result in cooperative or coupled gating and deviate from independent channel behavior. Using
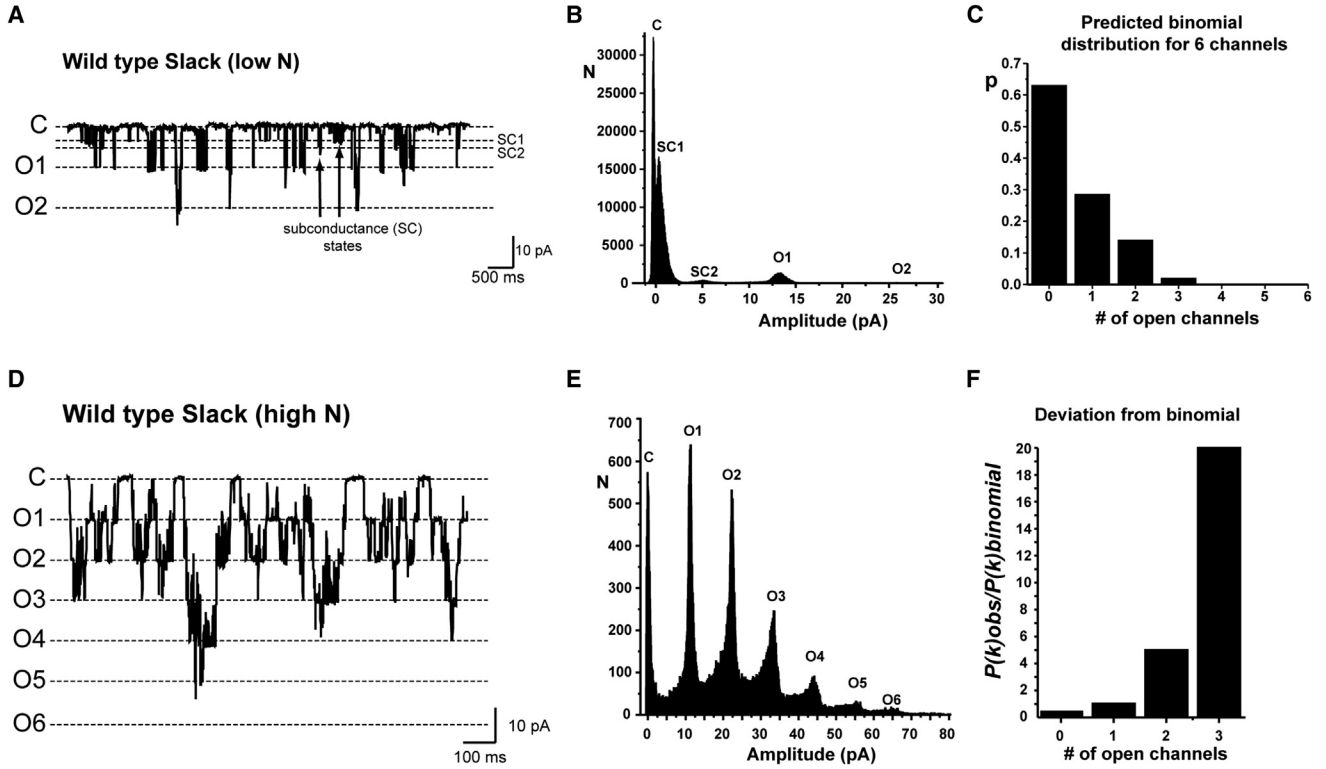
the single-channel Po obtained from the low-N all-points histogram (Figure 3B), we calculated the ratio of the observed Po at each level k, $P(k)_{obs}$, to the predicted distribution obtained from the binomial distribution, $P(k)_{binomial}$. This is plotted in Figure 3F for the first three levels of channel opening. If channel behaviors are the same in both types of patches, $P(k)_{obs}/P(k)_{binomial}$ should be ∼1 regardless of the number of channels present. The results show, however, that $P(k)_{obs}/P(k)_{binomial}$ increases with increasing k, suggesting a positive deviation from the binomial (Ding and Sachs, 2002).

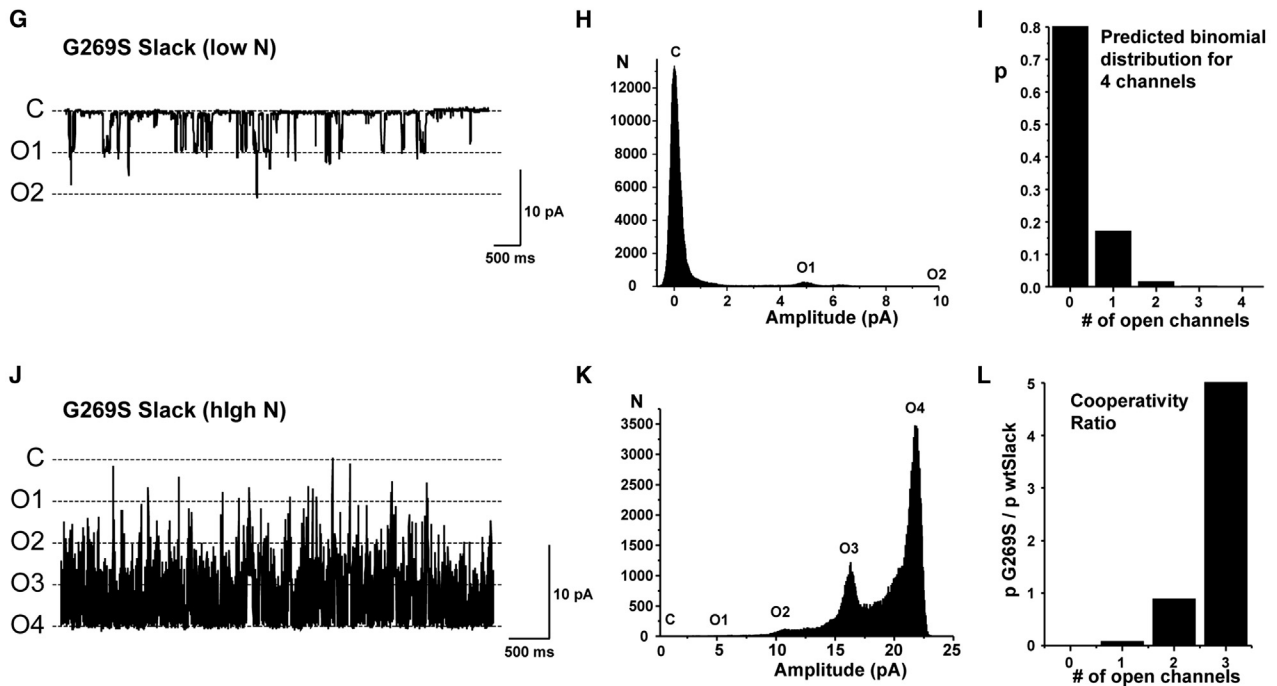**Positive Cooperativity Is Increased in the G269S Slack Channel**

The G269S Slack (hG288S) mutation has been found in both MMPSI and ADNFLE patients. Computational modeling of this mutation occurring in the S5 transmembrane domain has suggested that the introduction of a serine residue results in structural changes in the pore-forming region, which might lead to "impaired" channel function (Ishii et al., 2013). Given the nearly 10-fold increase in macroscopic current of the G269S mutation (Figures 1B and 1C), we were surprised that the unitary conductance of the channel was ∼80 pS, less than half that of WT Slack channels (∼180 pS) (Chen et al., 2009; Figures 3G and 3H).

As with the WT channels, we identified both low- and high-N on-cell patches of G269S channels. Figure 3G shows a trace with one channel predominantly open and rare simultaneous openings of a second channel. The all-points amplitude

Wild type Slack

A

Wild type Slack (low N)

B

C

Predicted binomial distribution for 6 channels

D

Wild type Slack (high N)

E

F

Deviation from binomial

G269S Slack

G

G269S Slack (low N)

H

I

Predicted binomial distribution for 4 channels

J

G269S Slack (high N)

K

L

Cooperativity Ratio

(legend on next page)

histogram in Figure 3H reflects the reduced unitary conductance and the fact that, like its WT counterpart, the channel is predominantly in the closed state. As a test of independence, we constructed a binomial distribution based on the probability of one channel opening (O1) in the low-N patch (Figure 3H) to calculate the expected distribution for four independently gating G269S channels (Figure 3I).

In sharp contrast to this prediction, recordings from a patch containing four G269S channels revealed multiple simultaneous openings, with very rare closings of all four channels (Figure 3J). Despite the fact that the predominant peak in the all-points histogram was for the simultaneous opening of all four channels, no opening of more than four channels was ever detected, indicating that only four functional channels were present in this patch (Figure 3K). However, the reduced unitary conductance observed in the low-N patches was unchanged in the high-N patches. This striking deviation of the experimental data from what was predicted by the binomial distribution suggests that cooperative gating of clusters of G269S channels increases their overall activity.

To quantify the difference in cooperativity between the G269S channel and WT Slack channels, we plotted a cooperativity ratio (the ratio of the observed Po at each level for G269S in high-N patches to the mean observed Po values for WT Slack in high-N patches [n = 4; Figure 3D]. If the degree of cooperativity were similar in both the mutant and WT channels in high-N patches, this ratio should be ~1 for each level of channel opening. Figure 3L shows, however, that there is an increase in the cooperativity ratio as the number of open channels increases, reflecting a dramatic increase in positive cooperativity for G269S.

Positive Cooperativity Is Increased in All of the Other Slack Mutants

We carried out similar analyses for all of the other mutations described in Table 1. All mutations other than G269S had unitary conductances in both low-N and high-N patches that were indistinguishable from those of WT Slack channels (n = 25 low-N patches, n = 13 high-N patches). In all cases, we found that the cooperativity ratio was increased compared with that in WT Slack channels. We provide figures of the data for two mutations in particular, the MMPSI R455H mutation and the OS

A945T mutation, which are located in the Regulator of Conductance for K 1 (RCK1) and RCK2 domains of the C terminus, respectively (Figure 1A).

In one of four low-N patches for the R455H channel, we recorded the activity of an apparently true single channel (Figure 4A). The Po of this channel was markedly increased compared with that in WT or G269S Slack, as evidenced by the relative size of the O1 peak in its amplitude histogram (Figure 4B) when compared with those in Figures 3B and 3H. As a result of this increased Po, the predicted peak of the amplitude distribution for five independent channels is no longer in the closed state (Figure 4C). However, recordings from a patch containing five R455H channels show that the distribution is shifted to the right over the predicted distribution (Figures 4D and 4E) and that the cooperativity is greater than that of WT Slack channels (Figure 4F), although by a smaller margin than the other mutations. This increased positive cooperativity was observed for all three high-N R455H patches.

Finally, for the A945T mutation, channel activity in low-N patches was low (n = 5; Figures 4G and 4H). As was also found for some other Slack mutants (R409Q and A913T; Barcia et al., 2012), SC states were absent or severely suppressed in the A945T mutant. The observed distribution of openings in a patch containing six channels, in which openings to a seventh level were never observed (Figures 4J and 4K), is substantially right-shifted compared with that predicted by the binomial distribution for independently gating low-N channels (Figure 4I). In sharp contrast to the prediction, simultaneous closing of all channels in three high-N patches of A945T channels was observed only very rarely. As a result, we conclude that positive cooperativity is very much greater in the A945T mutant than in WT Slack channels (Figure 4L).

DISCUSSION

Including the three new patients reported here, 31 epilepsy patients have now been shown to carry a *KCNT1* mutation (Barcia et al., 2012; Allen et al., 2013; Heron et al., 2012; Ishii et al., 2013; Martin et al., 2014; McTague et al., 2013; Vanderver et al., 2014). Although the manifestation of seizures differs among these patients, the occurrence of intellectual disability is notably high.

Figure 3. Single-Channel Recordings of WT and G269S Slack in *Xenopus* Oocytes

(A and B) Representative on-cell single-channel "low-N" trace recorded at −80 mV (A) and the corresponding all-points amplitude histogram (B). C, closed state; O1, one channel opening; O2, two channel openings. SC1 and SC2 indicate the two prominent subconductance states.

(C) Binomial distribution for six channels based on the single-channel Po in low-N patches (mean of eight low-N patches).

(D) Representative on-cell high-N patch recorded at −80 mV.

(E) All-points amplitude histogram of currents from (D). Experimental data show the increased frequency of multiple channel openings and dramatic reduction in dwell time in the fully closed state compared with the expected binomial distribution in (C).

(F) Deviation from binomial distribution. The plot shows the ratio of the observed Po at each level, P(k)$_{obs}$, to the predicted distribution obtained from the binomial distribution (C), P(k)$_{binomial}$, for the first three levels. The ratios continued to increase with successive k for four, five, and six channels (not shown).

(G and H) Representative on-cell, single-channel low-N trace of G269S channels at −80 mV (G) and the corresponding all-points amplitude histogram (H), representing 2 min of recording.
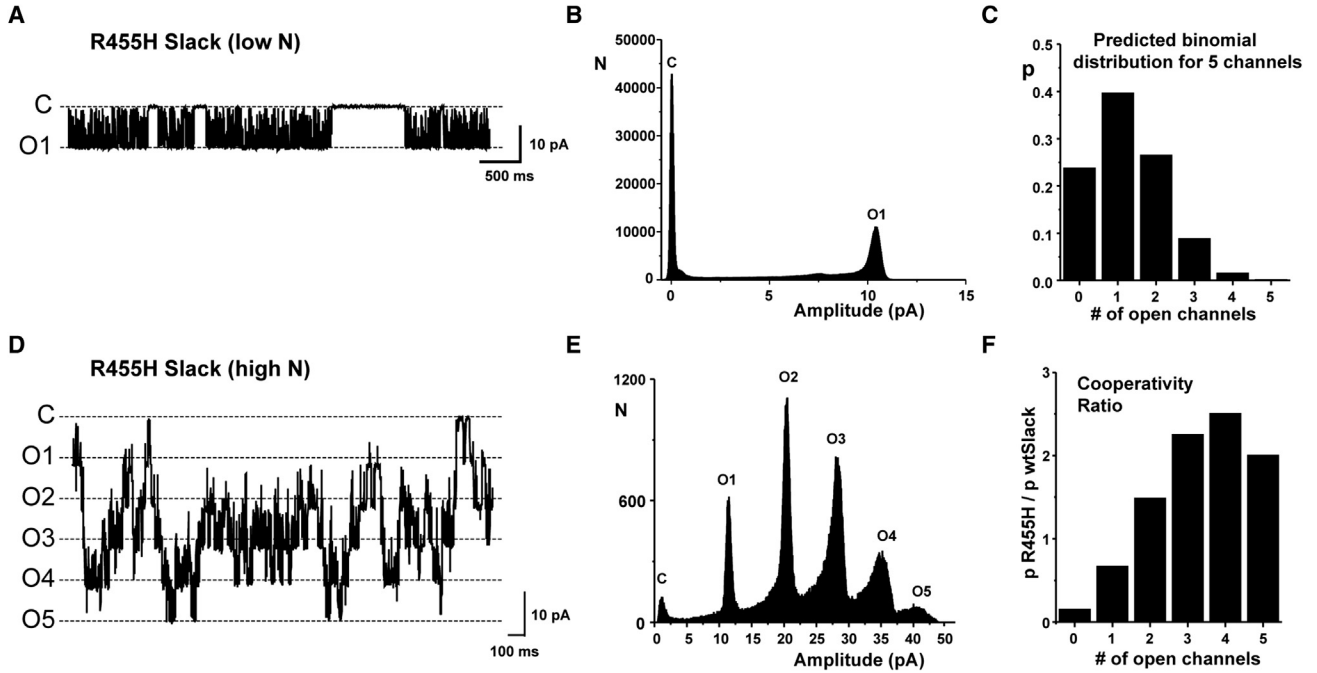
(I) Binomial distribution for four channels based on the mean single-channel Po in low-N patches (n = 4 low-N patches).

(J and K) Representative on-cell high-N patch containing four G269S channels (J) and the corresponding all-points amplitude histogram (K), showing a dramatically increased frequency of multiple channel openings compared with the expected binomial distribution (I).
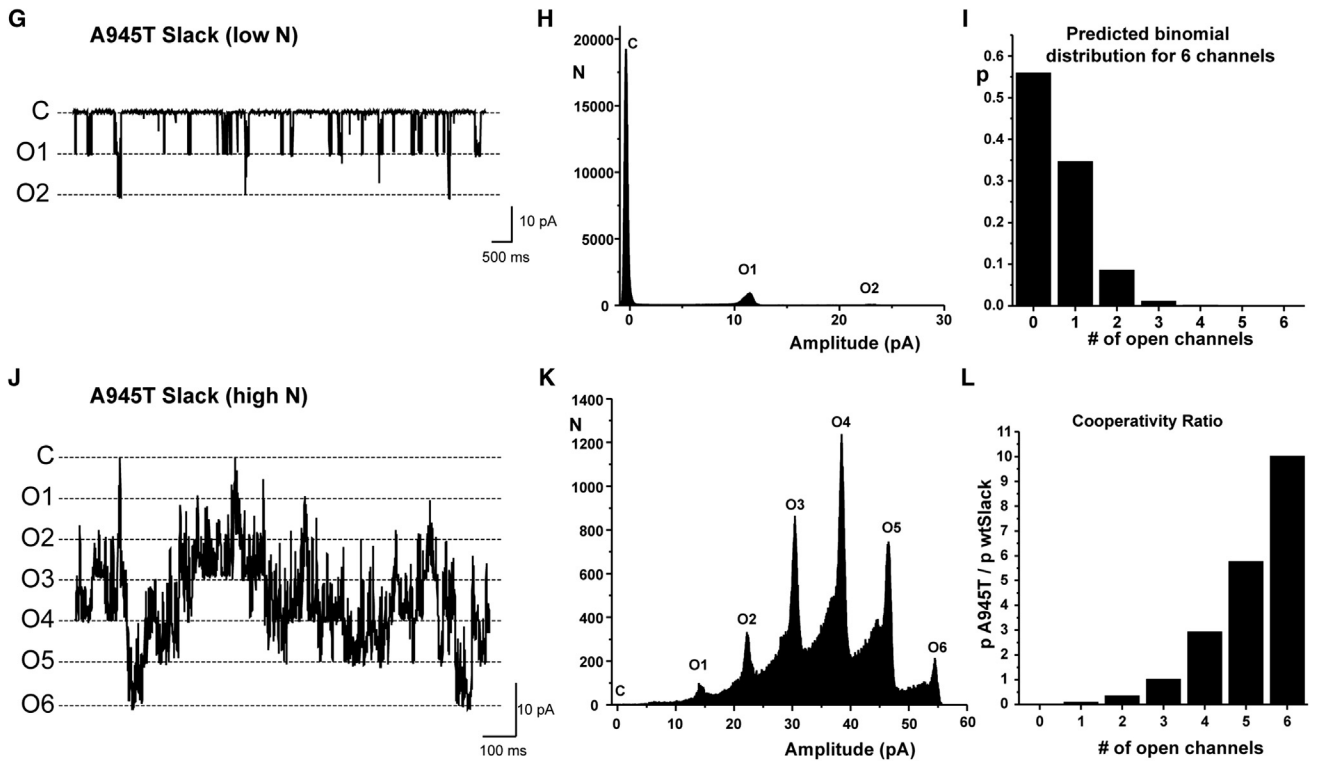
(L) Cooperativity ratio comparing P(k)$_{obs}$ for G269S versus WT Slack. The ratios were calculated from the means of four and five high-N patches for G269S and WT Slack, respectively. The ratios show a deviation from the expected value of one for each successive k, demonstrating increased positive cooperativity relative to WT Slack. The ratio for four open channels is 53 (not shown).

R455H Slack

A R455H Slack (low N)

B

C Predicted binomial distribution for 5 channels

D R455H Slack (high N)

E

F Cooperativity Ratio

A945T Slack

G A945T Slack (low N)

H

I Predicted binomial distribution for 6 channels

J A945T Slack (high N)

K

L Cooperativity Ratio

(legend on next page)

We observed an increase in channel activity for all nine mutants examined in our study, confirming previous studies (Barcia et al., 2012; Martin et al., 2014; Milligan et al., 2014), and documented this for the mutations hG288S and hR474H (rG269S and rR455H, respectively). We made the unexpected observation that WT Slack channels show positive cooperative gating, and gating of multiple channels deviates significantly from that predicted by the behavior of independent single channels. Moreover, each mutant channel had substantially greater cooperativity than the WT channel. Other non-disease-associated mutations in the C terminus, introduced for structure-function studies, display no gain of function (Barcia et al., 2012; Zhang et al., 2010). Thus, our observations provide a likely explanation for why the mutant channels produce greatly enhanced currents, and reveal a pathophysiological mechanism that may be at work in affected epilepsy patients. It is probable that the enhanced cooperativity is an intrinsic property of these mutations and will be detected in human neurons bearing these mutations. Definitive proof of this for Slack channels, however, may have to await studies on human tissue or potentially on animal models of Slack-associated diseases.

In our studies, the amplitude histograms for "low-N" patches were dominated by a single peak corresponding to the closed state, with only very rare simultaneous openings of more than one channel. As a result, in many cases it was not possible to be certain of the exact number of channels in the patch. Because single-channel Po values were calculated from such low-N patches, this method could have only overestimated the true single-channel Po and the calculated binomial distribution for openings for multiple independent channels. In contrast, the number of channels in high-N patches could be ascertained with greater confidence because of the increased Po together with the complete absence of openings above a fixed number of channels. In all cases, we found that Po was greatly enhanced in the high-N patches, despite the fact that in theory, such patches could contain, in addition to coupled channels, non-coupled channels that would dilute the degree of the cooperativity. Thus, of necessity, our calculations underestimate the true degree of cooperativity.

Cooperative gating was particularly striking for the MMPSI- and ADNFLE-associated G269S (hG288S) mutation in the S5 segment of Slack. A recent study using computational in silico modeling suggested that this mutation could impair channel function by introducing a new hydrogen bond that would alter the structure of the inner surface of the pore region (Ishii et al., 2013). The finding that the unitary conductance of the G269S channel was reduced (∼80 pS) is consistent with decreased throughput of potassium ions through the pore. Nevertheless, strongly augmented cooperative gating in this mutant increased macroscopic currents by ∼10-fold over those of WT Slack.

Our finding of one to three channels in low-Po patches and four or more in high-activity patches is consistent with what others have reported for cooperatively gating channels (Molina et al., 2006; Navedo et al., 2010). The colocalized spatial distribution or "clustering" of ion channels in specific cellular regions of neurons has been shown to be a necessary determinant of neuronal excitability (Vacher and Trimmer, 2012). In addition, a functional coupling of channels in a physical cluster, where the gating of one channel is directly coupled to the gating of neighboring channels, has been observed in a number of ion channel types at the single-channel level, including KcsA (Molina et al., 2006), Na^+ (Naundorf et al., 2006), Ca^{2+} (Navedo et al., 2010), Kir 4.1 (Horio et al., 1997), AMPA (Vaithianathan et al., 2005), HCN (Dekker and Yellen, 2006), $P2X_2$ (Ding and Sachs, 2002), CFTR (Krouse and Wine, 2001), and ryanodine receptors (Laver et al., 2004; Marx et al., 1998, 2001). A recent study reported increased positive cooperative gating in L-type Ca^{2+} channels during hypertension and Timothy syndrome (Navedo et al., 2010). We observe that a cohort of seemingly unrelated mutations in one channel can increase cooperativity gating behavior.

Our results also indicate that the degree to which $KCNT1$ mutations increase current amplitude in an expression system cannot readily be correlated with the clinical phenotype. MMPSI, with its signature early onset and pharmacoresistance, is more detrimental than ADNFLE. Across MMPSI mutants, increases in current compared with WT Slack ranged from 3- to 22-fold. Consistent with earlier suggestions (Milligan et al., 2014), increases for ADNFLE mutations were slightly smaller, ranging from 1.5- to 11-fold. Nevertheless, a small (3-fold) increase in Slack channel activity could lead to MMPSI (rR409Q), and a greater increase (11-fold) could produce the less severe condition of ADNFLE (rY775I).

Earlier studies found distinct de novo or germline mutations in MMPSI, ADNFLE, or OS patients, and in some cases the same mutation was found in multiple patients with the same diagnosis (Barcia et al., 2012; Heron et al., 2012; Ishii et al., 2013). This raised the possibility that there is a correlation between the location of a particular mutation in the channel protein and the type of epilepsy (Milligan et al., 2014). Our patient cohort suggests otherwise, as unrelated patients carried an identical mutation in $KCNT1$ even though they had been diagnosed with different types of epilepsy prior to their DNA sequencing. For example, patients 8 and 9, diagnosed with MMPSI (Ishii et al., 2013), and patient 10, an ADNFLE patient, all carried the mutant hG288S

Figure 4. Single-Channel Recordings of Slack Mutants R455H and A945T in *Xenopus* Oocytes

(A and B) Representative on-cell single-channel trace recorded at −80 mV from a patch expressing Slack R455H (A) and the corresponding all-points amplitude histogram (B).

(C) Binomial distribution for five R455H channels based on the mean single-channel Po from four low-N R455H patches.

(D and E) Representative high-N trace (D) and all-points amplitude histogram (E) from a patch containing five Slack R455H channels.

(F) Cooperativity ratios (comparing P(k)$_{obs}$ for R455H versus WT Slack) were calculated from the means of three and five high-N patches for G455R and WT Slack, respectively. The ratio shows a significant deviation from the expected value of one for all five channel openings.

(G and H) Representative low-N recording (G) and corresponding all-points amplitude histogram (H) from a patch containing A945T channels −80 mV.

(I) Binomial distribution for six channels based on the mean single-channel Po in low-N A945T patches (n = 5 low-N patches).

(J and K) Representative high-N recording (J) and corresponding all-points amplitude histogram (K) from patches containing six A945T channels.

(L) Cooperativity ratio as calculated from the means of three and five high-N patches for A945T and WT Slack, respectively.

(Table 1). In addition, hR398Q, a mutation that is known to be associated with familial ADNFLE (Heron et al., 2012), can also lead to MMPSI, as in patient 11. A misdiagnosis of epilepsy types in these patients is highly unlikely because MMPSI and ADNFLE are clinically distinct and differ in age of onset, type of seizures, and EEG pattern (Coppola et al., 1995; Scheffer et al., 1995). Our finding that *KCNT1* variants are associated with multiple different epilepsies is similar to previous observations in the sodium channel *SCN1A* (Escayg et al., 2000; Lossin, 2009; Oliva et al., 2012).

Human mutations of K$^+$ channels that increase neuronal excitability typically reduce K$^+$ currents (Ryan and Ptácek, 2010). How does a gain of function in Slack channels lead to epileptic seizures? Slack channels contribute to the delayed outward current, I$_{KNa}$ (Budelli et al., 2009), which helps to regulate neuronal excitability and adaptability in response to high-frequency stimulation (Bhattacharjee and Kaczmarek, 2005; Brown et al., 2008; Kaczmarek, 2013; Wallén et al., 2007). Increases in I$_{KNa}$ within a neuron, produced by enhanced cooperativity and/or by negative shifts in voltage dependence, would therefore be expected to reduce its excitability. There are at least four conditions, however, in which increases in I$_{KNa}$ could enhance the excitability of a network. First, an increased rate of action potential repolarization due to increased K$^+$ current attenuates Na$^+$ channel inactivation and promotes high-frequency firing, as is the case for Kv3 family K$^+$ channels (Brown and Kaczmarek, 2011). Second, a selective reduction in the excitability of inhibitory interneurons would enhance overall cortical excitability (Zhang et al., 2010). Third, changes in action potential firing during neuronal development could produce aberrant patterns of neuronal connectivity that lead to local epileptic foci (Katz and Shatz, 1996). Finally, the very severe outcomes of mutations in Slack could occur because they alter other biochemical interactions of the channel with its cytoplasmic partners (Brown et al., 2010; Huang et al., 2013). As has been reported for some other ion channels (Deng et al., 2013; Ferron et al., 2014), the large C-terminal cytoplasmic domain of Slack interacts with the fragile X mental retardation protein (FMRP), as well as its cargo mRNAs (Brown et al., 2010). Thus, in addition to directly altering the excitability of central neurons, mutations in Slack could disrupt intracellular signaling related to FMRP and activity-dependent protein translation.

EXPERIMENTAL PROCEDURES

Patients

Informed consent was obtained in accordance with the ethical standards of the Institutional Review Board on Human Experimentation of the Necker-Enfants Malades Hospital (Paris, France). Sixteen patients with *KCNT1* mutations were examined in this study. Thirteen of the patients had been reported previously. Of these, nine were diagnosed with MMPSI (Barcia et al., 2012; Ishii et al., 2013; McTague et al., 2013), three were diagnosed with ADNFLE (Heron et al., 2012), and one was diagnosed with OS (Martin et al., 2014). Two of the new patients had MMPSI and one had frontal epilepsy with a more severe outcome (in terms of both epilepsy pharmacoresistance and cognition) than ADNFLE (Table 1). We used previously reported methods, including whole exome sequencing (MMPSI and ADNFLE) and genome sequencing (OS) (Barcia et al., 2012; Heron et al., 2012; Martin et al., 2014), to identify *KCNT1* mutations causative for epilepsy syndromes. Mutation analysis of *KCNT1* in these patients was carried out as described below.

Mutation Analysis

KCNT1 exons were amplified by PCR from DNA extracted from venous blood, using flanking intronic primers. Sequence products were run on ABI 3730 automated sequencer (Applied Biosystems) and analyzed with SeqScqpe 2.5 (Applied Biosystem). Site-directed mutagenesis of the rat Slack-B construct was performed as previously described (Barcia et al., 2012) and mutations were confirmed by DNA sequencing.

Electrophysiological Characterization in *Xenopus* Oocytes

KCNT1 channels were characterized in oocytes injected with 10 ng of cRNA as described previously (Barcia et al., 2012). For whole-oocyte, two-electrode, voltage-clamp experiments, electrodes were filled with 3 M KCl and had resistances of 0.1–1.0 MΩ. The bath solution, MND-96, contained (in mM) 88 NaCl, 1 KCl, 2 MgCl$_2$, 1.8 CaCl$_2$, 5 glucose, 5 HEPES, 5 sodium pyruvate, and 50 μg/μl gentamicin (GIBCO; pH 7.4). For measurements of channel activation, oocytes were depolarized by 400 ms pulses from a holding potential of −80 mV to test voltages between −80 mV and +60 mV in 20 mV increments every 5 s.

For patch-clamp recording, cRNA-injected oocytes were manually devitellinized in a hypertonic solution containing (in mM) 220 Na$^+$ aspartate, 10 KCl, 2 MgCl$_2$, and 10 HEPES. On-cell patch recordings were performed using a symmetrical high-K$^+$ internal pipette and bath solutions consisting of (in mM) 100 K-gluconate, 40 KCl, 20 NaCl, 1 MgCl$_2$, 1 CaCl$_2$, 5 EGTA and 10 HEPES (pH 7.6). Hence, patch potentials in the text refer to the expected physiological potential difference across the membrane (i.e., −80 mV represents hyperpolarization). Although we carried out our analysis using stable cell-attached patches, we routinely observed that enhanced cooperativity persisted after the patches were excised from the cells. However, to avoid the potential rundown of channel activity that is known to occur for many channels following excision, we did not analyze the excised patches.

Protein Analysis

Crude membrane fractions were isolated from oocytes (Bröer, 2003). Protein samples (40 μg), separated on a 4%–15% gradient SDS gel and transferred to nitrocellulose paper, were probed overnight at 4°C with primary antibody as indicated. We used chicken anti-Slack IgY (1:5,000; Bhattacharjee et al., 2002), rabbit anti-Na$^+$/K$^+$ ATPase IgG (1:1,000; #3010; Cell Signaling), and horse anti-mouse (#PI-2000; Vector Labs) or goat anti-rabbit (#7074; Cell Signaling) horseradish peroxidase-conjugated secondary antibodies. Densitometry values from developed and imaged blots were determined using ImageJ.

Statistical Analysis

Data recording and analysis were performed using pClamp (Molecular Devices), Origin (Microsoft), and Prism (GraphPad). The average ± SEM values are plotted. When two groups were compared, two-tailed Student's t test was performed to determine statistical significance. When three or more groups were compared, one-way ANOVA followed by Bonferroni's post hoc test was performed unless indicated otherwise.

AUTHOR CONTRIBUTIONS

G.E.K. designed and performed whole-oocyte electrophysiological and western blot experiments. J.K. designed and performed single-channel electrophysiological experiments. G.B. and H.C.M. performed mutational analysis of patients' DNA samples. I.H.Q. performed electrophysiological experiments. L.C. performed mutagenesis experiments. E.B., J.C.T., O.D., and R.N. supervised clinical portions of the study. L.K.K. supervised the electrophysiological experiments. G.E.K., J.K., R.N., and L.K.K. jointly wrote the manuscript.

ACKNOWLEDGMENTS

REFERENCES

Allen, A.S., Berkovic, S.F., Cossette, P., Delanty, N., Dlugos, D., Eichler, E.E., Epstein, M.P., Glauser, T., Goldstein, D.B., Han, Y., et al.; Epi4K Consortium; Epilepsy Phenome/Genome Project (2013). De novo mutations in epileptic encephalopathies. Nature 501, 217–221.

Barcia, G., Fleming, M.R., Deligniere, A., Gazula, V.R., Brown, M.R., Langouet, M., Chen, H., Kronengold, J., Abhyankar, A., Cilio, R., et al. (2012). De novo gain-of-function KCNT1 channel mutations cause malignant migrating partial seizures of infancy. Nat. Genet. 44, 1255–1259.

Bhattacharjee, A., and Kaczmarek, L.K. (2005). For K+ channels, Na+ is the new Ca2+. Trends Neurosci. 28, 422–428.

Bhattacharjee, A., Gan, L., and Kaczmarek, L.K. (2002). Localization of the Slack potassium channel in the rat central nervous system. J. Comp. Neurol. 454, 241–254.

Bröer, S. (2003). Xenopus laevis Oocytes. Methods Mol. Biol. 227, 245–258.

Brown, M.R., and Kaczmarek, L.K. (2011). Potassium channel modulation and auditory processing. Hear. Res. 279, 32–42.

Brown, M.R., Kronengold, J., Gazula, V.R., Spilianakis, C.G., Flavell, R.A., von Hehn, C.A., Bhattacharjee, A., and Kaczmarek, L.K. (2008). Amino-termini isoforms of the Slack K+ channel, regulated by alternative promoters, differentially modulate rhythmic firing and adaptation. J. Physiol. 586, 5161–5179.

Brown, M.R., Kronengold, J., Gazula, V.R., Chen, Y., Strumbos, J.G., Sigworth, F.J., Navaratnam, D., and Kaczmarek, L.K. (2010). Fragile X mental retardation protein controls gating of the sodium-activated potassium channel Slack. Nat. Neurosci. 13, 819–821.

Budelli, G., Hage, T.A., Wei, A., Rojas, P., Jong, Y.J., O'Malley, K., and Salkoff, L. (2009). Na+-activated K+ channels express a large delayed outward current in neurons during normal physiology. Nat. Neurosci. 12, 745–750.

Chen, H., Kronengold, J., Yan, Y., Gazula, V.R., Brown, M.R., Ma, L., Ferreira, G., Yang, Y., Bhattacharjee, A., Sigworth, F.J., et al. (2009). The N-terminal domain of Slack determines the formation and trafficking of Slick/Slack heteromeric sodium-activated potassium channels. J. Neurosci. 29, 5654–5665.

Coppola, G., Plouin, P., Chiron, C., Robain, O., and Dulac, O. (1995). Migrating partial seizures in infancy: a malignant disorder with developmental arrest. Epilepsia 36, 1017–1024.

Dekker, J.P., and Yellen, G. (2006). Cooperative gating between single HCN pacemaker channels. J. Gen. Physiol. 128, 561–567.

Deng, P.Y., Rotman, Z., Blundon, J.A., Cho, Y., Cui, J., Cavalli, V., Zakharenko, S.S., and Klyachko, V.A. (2013). FMRP regulates neurotransmitter release and synaptic information transmission by modulating action potential duration via BK channels. Neuron 77, 696–711.

Ding, S., and Sachs, F. (2002). Evidence for non-independent gating of P2X2 receptors expressed in Xenopus oocytes. BMC Neurosci. 3, 17.

Escayg, A., MacDonald, B.T., Meisler, M.H., Baulac, S., Huberfeld, G., An-Gourfinkel, I., Brice, A., LeGuern, E., Moulard, B., Chaigne, D., et al. (2000). Mutations of SCN1A, encoding a neuronal sodium channel, in two families with GEFS+2. Nat. Genet. 24, 343–345.

Ferron, L., Nieto-Rostro, M., Cassidy, J.S., and Dolphin, A.C. (2014). Fragile X mental retardation protein controls synaptic vesicle exocytosis by modulating N-type calcium channel density. Nat Commun 5, 3628.

Heron, S.E., Smith, K.R., Bahlo, M., Nobili, L., Kahana, E., Licchetta, L., Oliver, K.L., Mazarib, A., Afawi, Z., Korczyn, A., et al. (2012). Missense mutations in the sodium-gated potassium channel gene KCNT1 cause severe autosomal dominant nocturnal frontal lobe epilepsy. Nat. Genet. 44, 1188–1190.

Horio, Y., Hibino, H., Inanobe, A., Yamada, M., Ishii, M., Tada, Y., Satoh, E., Hata, Y., Takai, Y., and Kurachi, Y. (1997). Clustering and enhanced activity of an inwardly rectifying potassium channel, Kir4.1, by an anchoring protein, PSD-95/SAP90. J. Biol. Chem. 272, 12885–12888.

Huang, F., Wang, X., Ostertag, E.M., Nuwal, T., Huang, B., Jan, Y.N., Basbaum, A.I., and Jan, L.Y. (2013). TMEM16C facilitates Na(+)-activated K+ currents in rat sensory neurons and regulates pain processing. Nat. Neurosci. 16, 1284–1290.

Ishii, A., Shioda, M., Okumura, A., Kidokoro, H., Sakauchi, M., Shimada, S., Shimizu, T., Osawa, M., Hirose, S., and Yamamoto, T. (2013). A recurrent KCNT1 mutation in two sporadic cases with malignant migrating partial seizures in infancy. Gene 531, 467–471.

Joiner, W.J., Tang, M.D., Wang, L.Y., Dworetzky, S.I., Boissard, C.G., Gan, L., Gribkoff, V.K., and Kaczmarek, L.K. (1998). Formation of intermediate-conductance calcium-activated potassium channels by interaction of Slack and Slo subunits. Nat. Neurosci. 1, 462–469.

Kaczmarek, L.K. (2013). Slack, Slick and sodium-activated potassium channels. ISRN Neurosci 2013, 354262.

Katz, L.C., and Shatz, C.J. (1996). Synaptic activity and the construction of cortical circuits. Science 274, 1133–1138.

Krouse, M.E., and Wine, J.J. (2001). Evidence that CFTR channels can regulate the open duration of other CFTR channels: cooperativity. J. Membr. Biol. 182, 223–232.

Laver, D.R., O'Neill, E.R., and Lamb, G.D. (2004). Luminal Ca2+-regulated Mg2+ inhibition of skeletal RyRs reconstituted as isolated channels or coupled clusters. J. Gen. Physiol. 124, 741–758.

Lossin, C. (2009). A catalog of SCN1A variants. Brain Dev. 31, 114–130.

Martin, H.C., Kim, G.E., Pagnamenta, A.T., Murakami, Y., Carvill, G.L., Meyer, E., Copley, R.R., Rimmer, A., Barcia, G., Fleming, M.R., et al.; WGS500 Consortium (2014). Clinical whole-genome sequencing in severe early-onset epilepsy reveals new genes and improves molecular diagnosis. Hum. Mol. Genet. 23, 3200–3211.

Marx, S.O., Ondrias, K., and Marks, A.R. (1998). Coupled gating between individual skeletal muscle Ca2+ release channels (ryanodine receptors). Science 281, 818–821.

Marx, S.O., Gaburjakova, J., Gaburjakova, M., Henrikson, C., Ondrias, K., and Marks, A.R. (2001). Coupled gating between cardiac calcium release channels (ryanodine receptors). Circ. Res. 88, 1151–1158.

McTague, A., Appleton, R., Avula, S., Cross, J.H., King, M.D., Jacques, T.S., Bhate, S., Cronin, A., Curran, A., Desurkar, A., et al. (2013). Migrating partial seizures of infancy: expansion of the electroclinical, radiological and pathological disease spectrum. Brain 136, 1578–1591.

Milligan, C.J., Li, M., Gazina, E.V., Heron, S.E., Nair, U., Trager, C., Reid, C.A., Venkat, A., Younkin, D.P., Dlugos, D.J., et al. (2014). KCNT1 gain of function in 2 epilepsy phenotypes is reversed by quinidine. Ann. Neurol. 75, 581–590.

Molina, M.L., Barrera, F.N., Fernández, A.M., Poveda, J.A., Renart, M.L., Encinar, J.A., Riquelme, G., and González-Ros, J.M. (2006). Clustering and coupled gating modulate the activity in KcsA, a potassium channel model. J. Biol. Chem. 281, 18837–18848.

Naundorf, B., Wolf, F., and Volgushev, M. (2006). Unique features of action potential initiation in cortical neurons. Nature 440, 1060–1063.

Navedo, M.F., Cheng, E.P., Yuan, C., Votaw, S., Molkentin, J.D., Scott, J.D., and Santana, L.F. (2010). Increased coupled gating of L-type Ca2+ channels during hypertension and Timothy syndrome. Circ. Res. 106, 748–756.

Oliva, M., Berkovic, S.F., and Petrou, S. (2012). Sodium channels and the neurobiology of epilepsy. Epilepsia 53, 1849–1859.

Ryan, D.P., and Ptácek, L.J. (2010). Episodic neurological channelopathies. Neuron 68, 282–292.

Scheffer, I.E., Bhatia, K.P., Lopes-Cendes, I., Fish, D.R., Marsden, C.D., Andermann, E., Andermann, F., Desbiens, R., Keene, D., Cendes, F., et al. (1995). Autosomal dominant nocturnal frontal lobe epilepsy. A distinctive clinical disorder. Brain 118, 61–73.

Vacher, H., and Trimmer, J.S. (2012). Trafficking mechanisms underlying neuronal voltage-gated ion channel localization at the axon initial segment. Epilepsia 53 (*Suppl 9*), 21–31.

Vaithianathan, T., Manivannan, K., Kleene, R., Bahr, B.A., Dey, M.P., Dityatev, A., and Suppiramaniam, V. (2005). Single channel recordings from synaptosomal AMPA receptors. Cell Biochem. Biophys. *42*, 75–85.

Vanderver, A., Simons, C., Schmidt, J.L., Pearl, P.L., Bloom, M., Lavenstein, B., Miller, D., Grimmond, S.M., and Taft, R.J. (2014). Identification of a novel de novo p.Phe932Ile KCNT1 mutation in a patient with leukoencephalopathy and severe epilepsy. Pediatr. Neurol. *50*, 112–114.

Wallén, P., Robertson, B., Cangiano, L., Löw, P., Bhattacharjee, A., Kaczmarek, L.K., and Grillner, S. (2007). Sodium-dependent potassium channels of a Slack-like subtype contribute to the slow afterhyperpolarization in lamprey spinal neurons. J. Physiol. *585*, 75–90.

Yuan, A., Santi, C.M., Wei, A., Wang, Z.W., Pollak, K., Nonet, M., Kaczmarek, L., Crowder, C.M., and Salkoff, L. (2003). The sodium-activated potassium channel is encoded by a member of the Slo gene family. Neuron *37*, 765–773.

Yuan, P., Leonetti, M.D., Pico, A.R., Hsiung, Y., and MacKinnon, R. (2010). Structure of the human BK channel Ca2+-activation apparatus at 3.0 A resolution. Science *329*, 182–186.

Zhang, Z., Rosenhouse-Dantsker, A., Tang, Q.Y., Noskov, S., and Logothetis, D.E. (2010). The RCK2 domain uses a coordination site present in Kir channels to confer sodium sensitivity to Slo2.2 channels. J. Neurosci. *30*, 7554–7562.